

# Theoretical uncertainties for measurements of $\alpha_s$ from electroweak observables

Hasko Stenzel  
II.Physikalisches Institut  
Justus-Liebig University of Giessen  
Heinrich-Buff Ring 16, D-35392 Giessen, Germany  
Hasko.Stenzel@cern.ch

## Abstract

One of the most precise measurements of the strong coupling constant  $\alpha_s(M_Z)$  is obtained in the context of global analyses of precision electroweak data. This article reviews the sensitivity of different electroweak observables to  $\alpha_s$  and describes the perturbative uncertainties related to missing higher orders. The complete renormalisation scale dependence for the relevant observables is calculated at next-to-next-to-leading order and a new method is presented to determine the corresponding perturbative uncertainty for measurements of  $\alpha_s$  based on these observables.

# 1 Introduction

High precision measurements of the parameters of the Standard Model (SM) have been carried out over the last 15 years in particular at LEP, SLC and TEVATRON. Cross sections, asymmetries, masses and widths of the electroweak (EW) gauge bosons have been determined with a relative accuracy of often better than one per mil. The measurements as a whole over-constrain the SM and allow for an internal consistency check. In a global fit to these data certain unknown parameters like the mass of Higgs boson can be determined, or other not directly measured quantities as the mass of the top quark can be inferred from the LEP data alone [1]. The sensitivity of the electroweak data to these parameters arise from higher order corrections.

The LEP and SLD experiments have carried out global SM fits to combined data from various experiments and determine five parameters simultaneously: the masses of the  $Z$  and Higgs bosons and of the top quark, the hadronic vacuum polarisation  $\Delta\alpha_{had}^{(5)}$  and the strong coupling constant  $\alpha_s(M_Z)$  constitute one often used set of parameters. The strong coupling constant plays a special role in these fits. It is essentially determined by hadronic observables, for which complete next-to-next-to-leading order (NNLO)  $\mathcal{O}(\alpha_s^3)$  calculations are available. The measurement of  $\alpha_s$  benefits from third order perturbative QCD calculation, which is not yet complete for other variables like jet rates, event shapes or fragmentation functions. The theoretical systematic uncertainties related to missing higher orders are expected to be smaller than for NLO-based determinations, even including all-orders resummation used for analyses of event-shape distributions [2].

The purpose of this article is a study of the intrinsic QCD uncertainties for a measurement of  $\alpha_s$  from electroweak observables. The experimental systematic uncertainties for  $\alpha_s$  are studied in detail by the LEP experiments as well as the correlation between  $\alpha_s$  and the other EW observables. A variation of the Higgs mass for example in the range from 100 to 1000 GeV entails a change in  $\alpha_s$  of about 0.0025, which has to be compared to an experimental uncertainty of  $\pm 0.0027$ .

This paper is organised as follows: in Section 2 the EW observables are briefly presented, in Section 3 the theoretical predictions for the widths, the effective couplings and the final state QCD corrections incorporated in the radiator functions are discussed. In Section 4 the theoretical uncertainties of the observables arising from the renormalisation scale variation are summarised, which are then used in Section 5 to assess the perturbative uncertainty for measurements of  $\alpha_s$  based on these observables. The conclusions are given in Section 6.

## 2 Electroweak observables

The sensitivity of certain electroweak observables to  $\alpha_s$  arises mainly through pure QCD corrections  $\mathcal{O}(\alpha_s^3)$  to the decay widths of the  $Z$  boson into hadronic final states. In addition, mixed QCD $\otimes$ EW corrections  $\mathcal{O}(\alpha\alpha_s)$  to the electroweak couplings give rise to a dependence of both hadronic and leptonic observables on  $\alpha_s$ . Numerically the former corrections amount to about three percent, while the mixed corrections, being suppressed by a factor of  $\alpha$ , are below one per mil. In practice only observables containing the

hadronic or total widths significantly contribute to the determination of  $\alpha_s$

$$\Gamma_h = \sum_q \Gamma_q, \quad \Gamma_q = \Gamma(Z \rightarrow q\bar{q}), \quad \Gamma_Z = \Gamma_h + \Gamma_l + \Gamma_\nu. \quad (1)$$

Beyond the width itself the  $R$  ratio

$$R_Z = \frac{\Gamma_h}{\Gamma_l}, \quad (2)$$

is of interest as the mixed corrections to the couplings cancel to a large extend in the ratio. For measurements of  $\alpha_s$  the most important observables are the leptonic and hadronic pole cross sections

$$\sigma_h^0 = 12\pi \frac{\Gamma_e \Gamma_h}{M_Z^2 \Gamma_Z^2}, \quad \sigma_l^0 = 12\pi \frac{\Gamma_e \Gamma_l}{M_Z^2 \Gamma_Z^2}. \quad (3)$$

In particular  $\sigma_l^0$  exhibits a good sensitivity to  $\alpha_s$  which allows a precise measurement of  $\alpha_s$  from this observable alone [1].

The calculations presented in this paper are carried out throughout with the electroweak library ZFITTER version 6.36 [3]. If not stated otherwise, the following numerical input values are used:

$$\begin{aligned} M_Z &= 91.1875 \text{ GeV} \\ m_t &= 175 \text{ GeV} \\ M_H &= 150 \text{ GeV} \\ \Delta\alpha_{had}^{(5)}(M_Z^2) &= 0.02761 \\ 1/\alpha(0) &= 137.0359895 \\ \alpha_s(M_Z) &= 0.1185 \end{aligned} \quad (4)$$

### 3 Partial widths

The dependence on  $\alpha_s$  and the renormalisation scale of the relevant EW observables through the widths are given in the following sections.

#### 3.1 Dependence of the widths on $\alpha_s$

The partial widths of the  $Z$  boson in a pair of fermions can be cast into two different expressions for leptons and quarks in order to incorporate the different types of radiative corrections. The width for lepton pairs  $l = e, \mu, \tau$  is given by:

$$\begin{aligned} \Gamma_l &= \Gamma_0 |\rho_Z^l| \sqrt{1 - \frac{4m_l^2}{M_Z^2}} \left( 1 + \frac{3}{4} \frac{\alpha(M_Z^2)}{\pi} Q_l^2 \right) \\ &\times \left[ \left( 1 + \frac{2m_l^2}{M_Z^2} \right) (1 + |g_Z^l|^2) - \frac{6m_l^2}{M_Z^2} \right], \end{aligned} \quad (5)$$

while for quark pairs  $q = u, d, s, c, b$  another expression is used:

$$\Gamma_q = \Gamma_0 C_F |\rho_Z^q| \left[ |g_Z^q|^2 R_V^q(M_Z^2) + R_A^q(M_Z^2) \right] + \Delta_{\text{EW/QCD}}. \quad (6)$$

The basic width  $\Gamma_0$  is the given by

$$\Gamma_0 = \frac{G_\mu M_Z^3}{24\sqrt{2}\pi} = 82.945(7) \text{ MeV}, \quad C_F = 3, \quad (7)$$

and  $C_F$  is a QCD QCD colour factor. In the case of leptons mass effect terms  $\propto \frac{m_l^2}{M_Z^2}$  are explicitly taken into account in Eq.5, for quarks these effects are embodied in the radiator functions  $R_V^q$  and  $R_A^q$ , which also account for QCD and QED radiative corrections. The core of the sensitivity of the widths and related EW observables to  $\alpha_s$  stems from the dependence of the radiator functions on  $\alpha_s$ , and their renormalisation scale dependence determines the theoretical uncertainty for a measurement of  $\alpha_s$ . The dependence of the widths and derived observables is depicted in figure 1, where the change of these quantities normalised to their value at  $\alpha_s(M_Z) = 0.1185$  is shown. For the leptonic widths a very small change below 0.1 per mill is observed, induced by two-loop corrections to the effective EW couplings and to the vacuum polarisation contribution to  $\alpha_{EM}$ . The hadronic widths exhibit a stronger and opposite dependence of about 3 per mill over the range of  $\alpha_s$  between 0.11 and 0.13, this dependence is induced by the radiator functions. Among the hadronic widths there are clear differences between up- and down-type quarks, the  $d$ - and the  $s$ -quark dependences are identical. Furthermore, finite mass quark effects entail small differences between the  $u$ - and the  $c$ -quark, more visible between the  $d$ -quark and the  $b$ -quark. The  $b$ -quark behaviour is accidentally very close, but not identical to the sum over all flavours.

The dependence of the EW observables on  $\alpha_s$  shown in figure 1 is, as for the widths, almost linear and up to three per mill in the considered range. The observable with the strongest dependence is  $\sigma_l^0$ , where the radiator functions enter quadratically in the denominator.

For quarks additional non-factorisable EW $\otimes$ QCD corrections  $\Delta_{EW/QCD}$  for the widths are not part of the radiator functions. These corrections are numerically very small (less than one per mill) and are taken as fixed numbers from [4, 5]

$$\begin{aligned} \Delta_{EW/QCD} &= -0.113 \text{ MeV } u-, c\text{-quarks} \\ &= -0.160 \text{ MeV } d-, s\text{-quarks} \\ &= -0.040 \text{ MeV } b\text{-quarks} \end{aligned} \quad (8)$$

The complex-valued variable  $\rho_Z^f$  measures the overall strength of the neutral current interaction in the  $f\bar{f}$  channel and the effective coupling  $g_Z^f$  can be expressed in terms of the ratio of effective vector and axial couplings

$$g_Z^f = \frac{v_f}{a_f} = 1 - 4|Q_f|(\kappa_Z^f s_W^2 + I_f^2), \quad (9)$$

where  $\kappa_Z^f$  defines an effective mixing angle for flavour  $f$  with  $s_W = \sin^2 \theta_W$  given by

$$s_W^2 = 1 - c_W^2, \quad c_W^2 = \frac{M_W^2}{M_Z^2} \quad (10)$$

The weak isospin  $I_f^{(3)}$  is  $\pm 1/2$  for up-/down-type quarks, the electric charge  $Q_f$  is  $+\frac{2}{3}/-\frac{1}{3}$  for up-/down-type quarks and  $I_f^2$  is given by

$$I_f^2 = \alpha^2(s) \frac{35}{18} \left[ 1 - \frac{8}{3} \text{Re}(\kappa_Z^f) s_W^2 \right]. \quad (11)$$

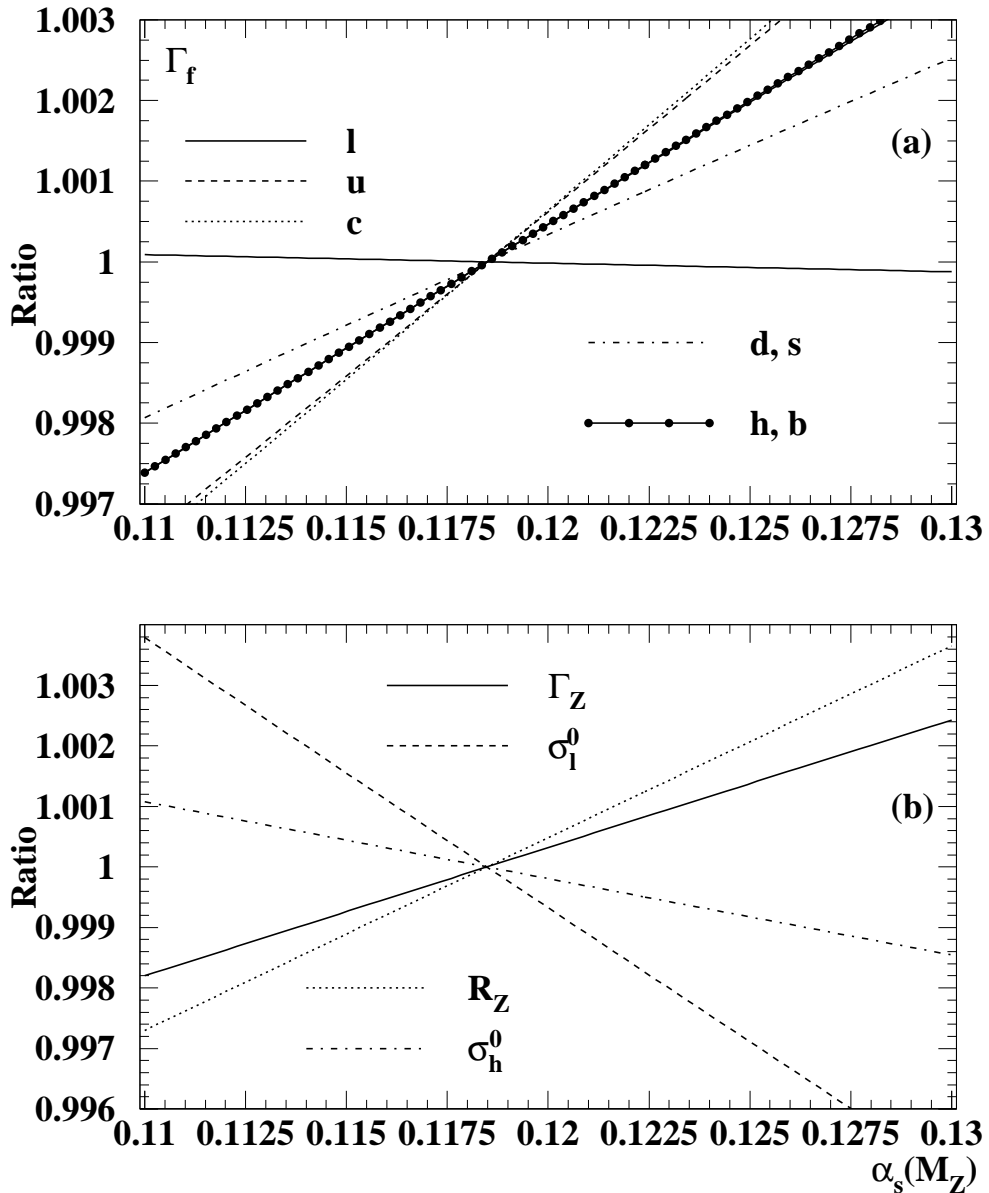


Figure 1: Dependence of the widths (a) and the EW observables (b) on  $\alpha_s(M_Z)$ . Shown is the normalised ratio of the observable to its reference value at  $\alpha_s(M_Z) = 0.1185$ . The other EW parameters are kept fixed to their nominal values.

The complex-valued effective couplings of the  $Z$  decay  $\kappa_Z^f$  and  $\rho_Z^q$  (in Eq.5,6) incorporate radiative electroweak corrections up to two loops and their full expressions are given in [3]. The factorisable EW $\otimes$ QCD corrections  $\mathcal{O}(\alpha\alpha_s)$  shall be studied here, as they induce the  $\alpha_s$  dependence to the effective couplings.

The running QED coupling denoted by  $\alpha(s)$  is given by:

$$\alpha(s) = \frac{\alpha(0)}{1 - \Delta\alpha_{had}^{(5)}(s) - \Delta\alpha_{lep}(s) - \Delta\alpha^t(s) - \Delta\alpha^{\alpha\alpha_s}(s)} . \quad (12)$$

The main contribution to the running coupling stems from the hadronic and leptonic

vacuum polarisation. The leptonic part has been calculated at third order [6]

$$\Delta\alpha_{lep}(M_z^2) = 0.03149767 , \quad (13)$$

with negligible uncertainties. The hadronic contribution of the five light flavours is related via the dispersion relation to  $R_\gamma$  (equivalent to  $R_Z$  in the continuum) from which it can be extracted [7]

$$\Delta\alpha_{had}^{(5)}(M_z^2) = 0.02761 \pm 0.0036 . \quad (14)$$

The contribution from the top quark is small but depends on the top quark mass, for  $m_t = 175$  GeV

$$\Delta\alpha^t(M_z^2) = -5.776 \cdot 10^{-5} . \quad (15)$$

An explicit dependence on  $\alpha_s$  appears in the  $\mathcal{O}(\alpha\alpha_s)$  correction, which has been calculated in [12]. It represents gluonic insertions in  $t\bar{t}$  loops. Of course the gluon exchange also occurs in light-quark loops and is accounted for in the experimental determination of  $\Delta\alpha_{had}^{(5)}$ . The correction for the top quark reads

$$\Delta\alpha^t(M_z^2) = -\frac{\alpha\alpha_s}{\pi^2} \frac{4}{9} \left( \text{Re} \left( \frac{V_1(r_Z)}{r_Z} \right) - 4\zeta(3) + \frac{5}{6} \right) , \quad r_Z = \frac{M_z^2 + i\epsilon}{4m_t^2} , \quad \zeta(3) = 1.2020569 , \quad (16)$$

where the expression for  $V_1(r)$  is given in [12]. The numerical value is

$$\Delta\alpha^{\alpha\alpha_s}(s) = -1.02 \cdot 10^{-5} . \quad (17)$$

The dependence of  $\alpha(s)$  on  $\alpha_s$  is very weak, its relative change is about  $10^{-6}$  for a variation of  $\alpha_s(M_z)$  between 0.11 and 0.13.

### 3.2 Effective electroweak couplings

The effective electroweak couplings  $\rho$  and  $\kappa$  contain various self-energy terms, calculated for the EW part at NLO with two-loop corrections, as well as mixed EW $\otimes$ QCD corrections. The expressions for EW part are given in [3], here only the terms relevant for the  $\alpha_s$  dependence are summarised. In a convenient decomposition  $\rho$  and  $\kappa$  are split into leading and remainder contributions, each being gauge invariant separately. The dominant leading term is re-summed to all orders in perturbation theory and the sub-leading remainder is calculated in fixed-order theory. The couplings  $\rho$  and  $\kappa$  can be expanded in the following combination of leading and remainder terms:

$$\rho_z^f = \frac{1 + f_\alpha (\rho_{rem}^{f,G} + \rho_{rem}^{f,G\alpha_s}) + \rho_{rem}^{f,G^2}}{1 + (\hat{\rho}^G + \hat{\rho}^{G\alpha_s}) (1 - \Delta r_{rem}^G - \Delta r_{rem}^{G\alpha_s})} , \quad (18)$$

$$\begin{aligned} \kappa_z^f &= \left[ 1 + f_\alpha (\kappa_{rem}^{f,G} + \kappa_{rem}^{f,G\alpha_s}) + \kappa_{rem}^{f,G^2} \right] \\ &\times \left[ 1 - \frac{c_W^2}{s_W^2} (\hat{\rho}^{f,G} + \hat{\rho}^{f,G\alpha_s}) (1 - \Delta r_{rem}^G - \Delta r_{rem}^{G\alpha_s}) \right] . \end{aligned} \quad (19)$$

The transformation factor  $f_\alpha$  accounts for the conversion of couplings  $\alpha \rightarrow G_\mu$  [18]

$$f_\alpha = \frac{\sqrt{2}G_\mu M_Z s_W^2 c_W^2}{\pi\alpha} . \quad (20)$$

The common leading term containing strong corrections is

$$\begin{aligned}\hat{\rho}^{G\alpha_s} &= 3x_t \left( c_{t1} \frac{\alpha_s(m_t)}{\pi} + c_{t2} \left( \frac{\alpha_s(m_t)}{\pi} \right)^2 \right), \\ x_t &= \frac{G_\mu m_t^2}{8\pi^2 \sqrt{2}}, \quad c_{t1} = -2.86, \quad c_{t2} = -18.18,\end{aligned}\quad (21)$$

where only the leading term in  $m_t^2$  is known for  $c_{t2}$  [8]. The expansions of  $\rho$  and  $\kappa$  have also the remainders of the renormalisation parameter  $\Delta r$  [3] in common, the component containing the QCD corrections is given by

$$\Delta r_{rem}^{G\alpha_s} = tb - tbl + 2cl, \quad (22)$$

$$tb = \frac{\alpha\alpha_s(m_t)}{\pi^2} dr_{rem}(M_Z, M_W, m_t^2), \quad (23)$$

$$tbl = \frac{\alpha\alpha_s(m_t)}{4\pi^2} \frac{m_t^2}{M_W^2} \frac{M_Z^2}{M_Z^2 - M_W^2} \left( \frac{1}{2} + \frac{\pi^2}{6} \right), \quad (24)$$

$$\begin{aligned}cl &= -\frac{\alpha\alpha_s(M_Z)}{4\pi^2} \frac{M_Z^2 M_W^2}{(M_Z^2 - M_W^2)^2} \log \left( \frac{M_W^2}{M_Z^2} \right) \\ &\quad \times \left[ 1 + c_{l1} \frac{\alpha_s(M_Z)}{\pi} + c_{l2} \left( \frac{\alpha_s(M_Z)}{\pi} \right)^2 \right],\end{aligned}\quad (25)$$

$$c_{l1} = 1.409, \quad c_{l2} = -12.805. \quad (26)$$

The QCD correction for the flavour-dependent remainder of  $\rho$  is

$$\rho_{rem}^{f,G\alpha_s} = \rho^{QCD} + tbl, \quad (27)$$

$$\begin{aligned}\rho^{QCD} &= \frac{\alpha\alpha_s(m_t)}{\pi^2} d\rho_{rem}(M_Z, M_W, m_t^2) \\ &\quad + \frac{\alpha\alpha_s(M_Z)}{\pi^2} \frac{V_T^2(t) + V_T^2(b) + 2}{8s_W^2 c_W^2},\end{aligned}\quad (28)$$

$$V_T(q) = 1 - 4Q_q s_W^2 \quad (29)$$

The expression for  $\kappa$  contains one different QCD correction for the remainder

$$\kappa_{rem}^{f,G\alpha_s} = \kappa^{QCD} + \frac{M_W^2}{M_Z^2 - M_W^2} tbl - 3x_t c_{a2} \left( \frac{\alpha_s(m_t)}{\pi} \right), \quad (30)$$

$$c_{a2} = 0.644, \quad (31)$$

$$\kappa^{QCD} = \frac{\alpha\alpha_s(m_t)}{\pi^2} d\kappa_{rem}(M_Z, M_W, m_t^2) \quad (32)$$

$$+ \frac{\alpha\alpha_s(M_Z)}{\pi^2} \frac{c_W^2}{2s_W^4} \log c_W^2 \quad (33)$$

The remainder functions  $dr_{rem}$ ,  $d\rho_{rem}$  and  $d\kappa_{rem}$  describing the  $\mathcal{O}(\alpha\alpha_s)$  contribution to the bosonic self-energies have been derived analytically in [12]. In the case of b quarks two additional one-loop vertex diagrams, absent in the case of light quarks, are generated by the large mass splitting between the t and the b quark and contribute to the widths

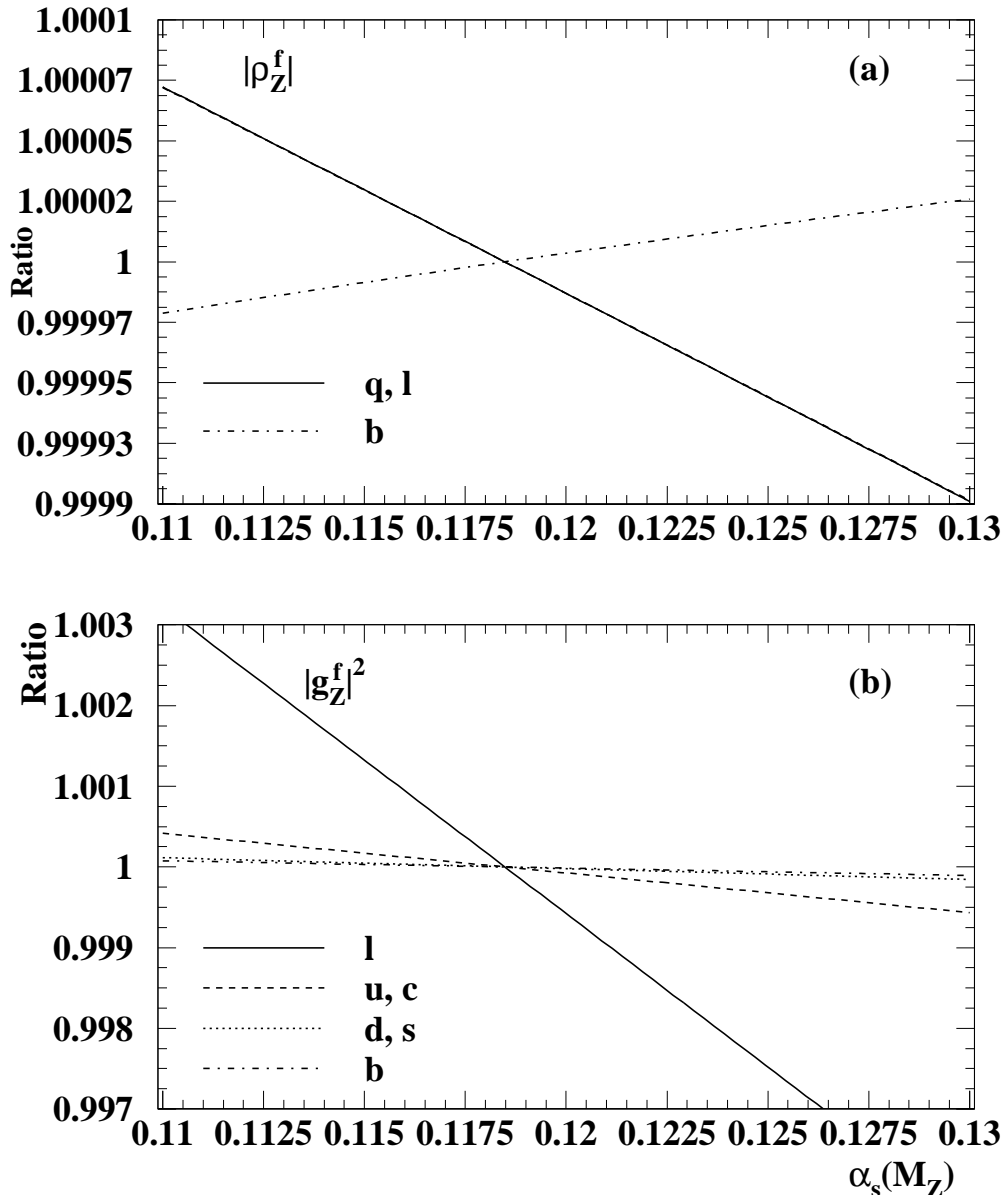


Figure 2: Dependence of the  $|\rho_Z^f|$  (a) and  $|g_Z^f|^2$  (b) on  $\alpha_s(M_Z)$ . Shown is the normalised ratio of the coupling to its reference value at  $\alpha_s(M_Z) = 0.1185$ .

$\Gamma_b$  [9]. These corrections entail a modification of the  $Zb\bar{b}$  decay amplitude form factor [3], which in turn affects the effective couplings. If  $\rho'$  and  $\kappa'$  denote the modified couplings given in [3], then the corrected couplings for the b quark are obtained by

$$\rho_Z^b = \rho' (1 + \tau_b)^2 , \quad (34)$$

$$\kappa_Z^b = \frac{\kappa'}{1 + \tau_b} , \quad (35)$$

$$\tau_b = -2x_t \left( 1 - \frac{\pi}{3} \alpha_s(m_t) + x_t \tau_2 \frac{m_t^2}{M_H^2} \right) , \quad (36)$$

where the term in  $\alpha_s(m_t)$  was obtained by [10] and an expression for  $\tau_2$  can be found in [11].

The dependence of the couplings on  $\alpha_s$  is shown in fig.2 for the absolute value of  $\rho_Z^f$  and the squared module of  $g_Z^f$ , these are the relevant forms for the widths according to Eqs.56. The dependence of  $\rho$  on  $\alpha_s$  is weak, the relative change in the range considered is below  $2 \cdot 10^{-4}$ . All quark flavours and the leptons exhibit practically the same  $\alpha_s$  dependence, except the b quark for which it is even weaker and opposite. In contrast to  $\rho$ , the  $\alpha_s$  dependence of  $g$  is much stronger. A change of about six per mill is observed for the leptons and less than 0.5 per mill for the quarks. The ranking of the dependence for leptons, u- and d-type quarks is determined by the electric charge, which enters quadratically in the expression Eq.9 for  $|g_Z^f|^2$ .

The observed  $\alpha_s$  dependence of the leptonic widths shown in fig. 1 is dominated by  $\rho$ 's dependence on  $\alpha_s$ . In the case of quarks, however, the couplings contribution to the  $\alpha_s$  dependence of the widths is sub-leading, the main properties are determined by the QCD final state corrections in the radiator functions.

### 3.3 Radiator functions

Final state QCD and QED vector and axial vector corrections to the quarkonic widths Eq.6 are embodied in the radiator functions

$$\begin{aligned}
R_V^q(s) = & 1 + \frac{3}{4} Q_q^2 \frac{\alpha(s)}{\pi} + \frac{\alpha_s(s)}{\pi} - \frac{1}{4} Q_q^2 \frac{\alpha(s)}{\pi} \frac{\alpha_s(s)}{\pi} \\
& + \left[ C_{02} + C_2^t \left( \frac{s}{m_t^2} \right) \right] \left( \frac{\alpha_s(s)}{\pi} \right)^2 + C_{03} \left( \frac{\alpha_s(s)}{\pi} \right)^3 \\
& + \frac{m_c^2(s) + m_b^2(s)}{s} C_{23} \left( \frac{\alpha_s(s)}{\pi} \right)^3 \\
& + \frac{m_q^2(s)}{s} \left[ C_{21}^V \frac{\alpha_s(s)}{\pi} + C_{22}^V \left( \frac{\alpha_s(s)}{\pi} \right)^2 + C_{23}^V \left( \frac{\alpha_s(s)}{\pi} \right)^3 \right] \\
& + \frac{m_c^4(s)}{s^2} \left[ C_{42} - \ln \frac{m_c^2(s)}{s} \right] \left( \frac{\alpha_s(s)}{\pi} \right)^2 + \frac{m_b^4(s)}{s^2} \left[ C_{42} - \ln \frac{m_b^2(s)}{s} \right] \left( \frac{\alpha_s(s)}{\pi} \right)^2 \\
& + \frac{m_q^4(s)}{s^2} \left\{ C_{41}^V \frac{\alpha_s(s)}{\pi} + \left[ C_{42}^V + C_{42}^{V,L} \ln \frac{m_q^2(s)}{s} \right] \left( \frac{\alpha_s(s)}{\pi} \right)^2 \right\} \\
& + 12 \frac{m_q'^4(s)}{s^2} \left( \frac{\alpha_s(s)}{\pi} \right)^2 - \frac{m_q^6(s)}{s^3} \left\{ 8 + \frac{16}{27} \left[ 155 + 6 \ln \frac{m_q^2(s)}{s} \right] \frac{\alpha_s(s)}{\pi} \right\}, \quad (37)
\end{aligned}$$

$$\begin{aligned}
R_A^q(s) = & 1 + \frac{3}{4} Q_q^2 \frac{\alpha(s)}{\pi} + \frac{\alpha_s(s)}{\pi} - \frac{1}{4} Q_q^2 \frac{\alpha(s)}{\pi} \frac{\alpha_s(s)}{\pi} \\
& + \left[ C_{02} + C_2^t \left( \frac{s}{m_t^2} \right) - (2I_q^{(3)}) \mathcal{I}^{(2)} \left( \frac{s}{m_t^2} \right) \right] \left( \frac{\alpha_s(s)}{\pi} \right)^2 \\
& + \left[ C_{03} - (2I_q^{(3)}) \mathcal{I}^{(3)} \left( \frac{s}{m_t^2} \right) \right] \left( \frac{\alpha_s(s)}{\pi} \right)^3 \\
& + \frac{m_c^2(s) + m_b^2(s)}{s} C_{23} \left( \frac{\alpha_s(s)}{\pi} \right)^3 + \frac{m_q^2(s)}{s} \left[ C_{20}^A + C_{21}^A \frac{\alpha_s(s)}{\pi} + C_{22}^A \left( \frac{\alpha_s(s)}{\pi} \right)^2 \right]
\end{aligned}$$

$$\begin{aligned}
& +6 \left( 3 + \ln \frac{m_t^2}{s} \right) \left( \frac{\alpha_s(s)}{\pi} \right)^2 + C_{23}^A \left( \frac{\alpha_s(s)}{\pi} \right)^3 \Big] \\
& - 10 \frac{m_q^2(s)}{m_t^2} \left[ \frac{8}{81} + \frac{1}{54} \ln \frac{m_t^2}{s} \right] \left( \frac{\alpha_s(s)}{\pi} \right)^2 \\
& + \frac{m_c^4(s)}{s^2} \left[ C_{42} - \ln \frac{m_c^2(s)}{s} \right] \left( \frac{\alpha_s(s)}{\pi} \right)^2 + \frac{m_b^4(s)}{s^2} \left[ C_{42} - \ln \frac{m_b^2(s)}{s} \right] \left( \frac{\alpha_s(s)}{\pi} \right)^2 \\
& + \frac{m_q^4(s)}{s^2} \left\{ C_{40}^A + C_{41}^A \frac{\alpha_s(s)}{\pi} + \left[ C_{42}^A + C_{42}^{A,L} \ln \frac{m_q^2(s)}{s} \right] \left( \frac{\alpha_s(s)}{\pi} \right)^2 \right\} \\
& - 12 \frac{m_q'^4(s)}{s^2} \left( \frac{\alpha_s(s)}{\pi} \right)^2. \tag{38}
\end{aligned}$$

Finite mass corrections are retained only for the  $b$ - and  $c$ -quark, i.e.  $m_q = 0$  for  $q = u, d, s$ , and the terms  $m_q(s)$  represent the running quark masses in the  $\overline{\text{MS}}$  scheme. The term  $m_q'$  denotes the other quark mass in doublet, it is  $m_c$  for  $q = b$  and  $m_b$  for  $q = c$ . The different terms of Eq.37 and Eq.38 and their coefficients can be organised in the following classes of corrections.

Massless non-singlet corrections [13, 14, 15, 16]:

$$C_{02} = \frac{365}{24} - 11 \zeta(3) + \left[ -\frac{11}{12} + \frac{2}{3} \zeta(3) \right] n_f, \tag{39}$$

$$\begin{aligned}
C_{03} = & \frac{87029}{288} - \frac{121}{8} \zeta(2) - \frac{1103}{4} \zeta(3) + \frac{275}{6} \zeta(5) \\
& + \left[ -\frac{7847}{216} + \frac{11}{6} \zeta(2) + \frac{262}{9} \zeta(3) - \frac{25}{9} \zeta(5) \right] n_f \\
& + \left[ \frac{151}{162} - \frac{1}{18} \zeta(2) - \frac{19}{27} \zeta(3) \right] n_f^2, \tag{40}
\end{aligned}$$

with the number of active flavours  $n_f$ .

Quadratic massive corrections [17]:

$$C_{23} = -80 + 60 \zeta(3) + \left[ \frac{32}{9} - \frac{8}{3} \zeta(3) \right] n_f, \tag{41}$$

$$C_{21}^V = 12, \tag{42}$$

$$C_{22}^V = \frac{253}{2} - \frac{13}{3} n_f, \tag{43}$$

$$\begin{aligned}
C_{23}^V = & 2522 - \frac{855}{2} \zeta(2) + \frac{310}{3} \zeta(3) - \frac{5225}{6} \zeta(5) \\
& + \left[ -\frac{4942}{27} + 34 \zeta(2) - \frac{394}{27} \zeta(3) + \frac{1045}{27} \zeta(5) \right] n_f + \left[ \frac{125}{54} - \frac{2}{3} \zeta(2) \right] n_f^2, \tag{44}
\end{aligned}$$

$$C_{20}^A = -6, \tag{45}$$

$$C_{21}^A = -22, \quad (46)$$

$$C_{22}^A = -\frac{8221}{24} + 57\zeta(2) + 117\zeta(3) + \left[ \frac{151}{12} - 2\zeta(2) - 4\zeta(3) \right] n_f, \quad (47)$$

$$\begin{aligned} C_{23}^A = & -\frac{4544045}{864} + 1340\zeta(2) + \frac{118915}{36}\zeta(3) - 127\zeta(5) \\ & + \left[ \frac{71621}{162} - \frac{209}{2}\zeta(2) - 216\zeta(3) + 5\zeta(4) + 55\zeta(5) \right] n_f \\ & + \left[ -\frac{13171}{1944} + \frac{16}{9}\zeta(2) + \frac{26}{9}\zeta(3) \right] n_f^2; \end{aligned} \quad (48)$$

Quartic massive corrections:

$$C_{42} = \frac{13}{3} - 4\zeta(3), \quad (49)$$

$$C_{40}^V = -6, \quad (50)$$

$$C_{41}^V = -22, \quad (51)$$

$$C_{42}^V = -\frac{3029}{12} + 162\zeta(2) + 112\zeta(3) + \left[ \frac{143}{18} - 4\zeta(2) - \frac{8}{3}\zeta(3) \right] n_f, \quad (52)$$

$$C_{42}^{V,L} = -\frac{11}{2} + \frac{1}{3}n_f, \quad (53)$$

$$C_{40}^A = 6, \quad (54)$$

$$C_{41}^A = 10, \quad (55)$$

$$C_{42}^A = \frac{3389}{12} - 162\zeta(2) - 220\zeta(3) + \left[ -\frac{41}{6} + 4\zeta(2) + \frac{16}{3}\zeta(3) \right] n_f, \quad (56)$$

$$C_{42}^{A,L} = \frac{77}{2} - \frac{7}{3}n_f; \quad (57)$$

Power suppressed t-quark mass correction:

$$C_2^t(x) = x \left( \frac{44}{675} - \frac{2}{135} \ln x \right); \quad (58)$$

Singlet axial corrections:

$$\mathcal{I}^{(2)}(x) = -\frac{37}{12} + \ln x + \frac{7}{81}x + 0.0132x^2, \quad (59)$$

$$\mathcal{I}^{(3)}(x) = -\frac{5075}{216} + \frac{23}{6}\zeta(2) + \zeta(3) + \frac{67}{18}\ln x + \frac{23}{12}\ln^2 x. \quad (60)$$

Here, the Riemann Zeta function  $\zeta$  is defined by

$$\zeta(x) = \sum_{n=1}^{\infty} n^{-x} \quad (61)$$

with particular values

$$\zeta(2) = 1.6449341, \quad \zeta(3) = 1.2020569, \quad \zeta(5) = 1.0369278. \quad (62)$$

The evolution of the radiator functions with  $\alpha_s$  is shown in fig.3. The vector radiator

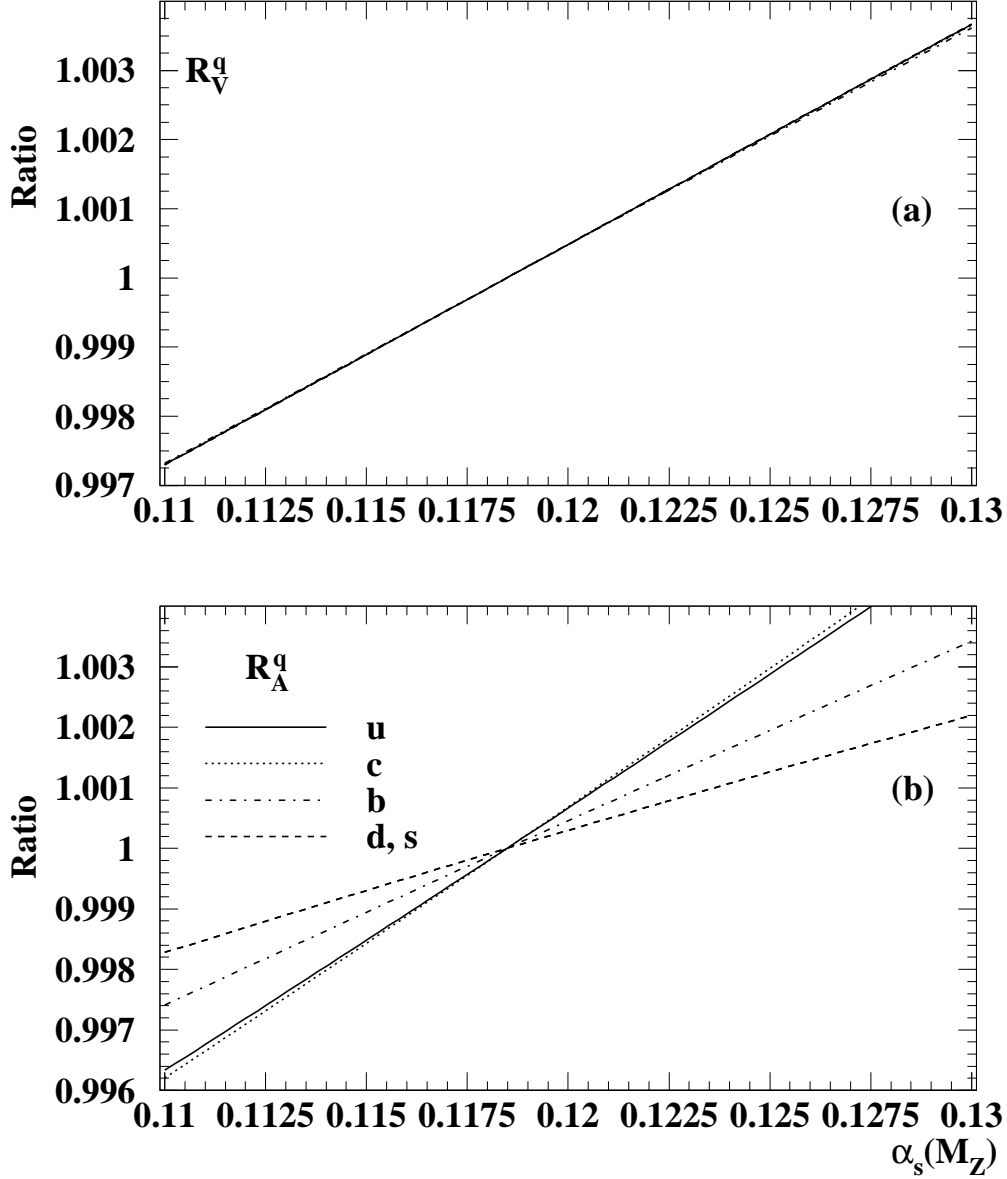


Figure 3: Dependence of the radiator functions  $R_V^q$  (a) and  $R_A^q$  (b) on  $\alpha_s(M_Z)$ . The ratio of the radiator function at a given value of  $\alpha_s(M_Z)$  and the reference value at  $\alpha_s(M_Z) = 0.1185$  is shown.

functions for the different flavours are very similar and can barely be distinguished. Their dependence on  $\alpha_s$  is almost linear and increasing by 0.6 % for a raise of  $\alpha_s$  from 0.11 to 0.13. The axial-vector radiator function exhibits a prominent flavour dependence. For up-type quarks  $R_A^q$  increases by 0.8%, for down-type quarks the change of the axial-vector radiator function is only of 0.4 %. The third component of the weak isospin  $I_q^{(3)}$  present in singlet axial component of  $R_A^q$  generates the up/down-quark difference. On top of this difference the b-quark mass corrections are important and entail a change of  $R_A^b$  by 0.6 %.

### 3.3.1 Running quark masses

The running quark masses  $m_q(s)$  in the  $\overline{\text{MS}}$  scheme are related to the fixed-valued pole masses  $M_q$ . For the  $c$ -quark at  $s = M_c^2$  and  $n_f = 4$  it follows

$$\begin{aligned} M_c &= m_c(M_c^2) \left\{ 1 + \left[ \frac{4}{3} + \ln \frac{M_c^2}{m_c^2(M_c^2)} \right] \frac{\alpha_s(M_c^2)}{\pi} \right. \\ &+ \left[ K_c + \left( \frac{173}{24} - \frac{13}{36} n_f \right) \ln \frac{M_c^2}{m_c^2(M_c^2)} + \left( \frac{15}{8} - \frac{1}{12} n_f \right) \ln^2 \frac{M_c^2}{m_c^2(M_c^2)} \right. \\ &\left. \left. + \frac{4}{3} \Xi \left( \frac{m_s(M_c^2)}{m_c(M_c^2)} \right) \right] \left( \frac{\alpha_s(M_c^2)}{\pi} \right)^2 \right\}, \end{aligned} \quad (63)$$

with

$$K_c = \frac{2905}{288} + \frac{1}{3} \left[ 7 + 2 \ln(2) \right] \zeta(2) - \frac{1}{6} \zeta(3) - \frac{1}{3} \left[ \frac{71}{48} + \zeta(2) \right] n_f, \quad (64)$$

$$\Xi(x) = \frac{\pi^2}{8} x - 0.597 x^2 + 0.23 x^3. \quad (65)$$

The running mass is evolved according to the renormalisation group equation from the scale of the pole mass  $M_c^2$  to the scale of the process  $s$  in a two-step evolution  $M_c^2 \rightarrow M_b^2 \rightarrow s$ :

$$\begin{aligned} m_c(s) &= m_c(M_c^2) \left[ \frac{\alpha_s(M_b^2)}{\alpha_s(M_c^2)} \right]^{\gamma_0^{(4)}/\beta_0^{(4)}} \left\{ 1 + C_1(4) \left[ \frac{\alpha_s(M_b^2)}{\pi} - \frac{\alpha_s(M_c^2)}{\pi} \right] \right. \\ &+ \frac{1}{2} C_1^2(4) \left[ \frac{\alpha_s(M_b^2)}{\pi} - \frac{\alpha_s(M_c^2)}{\pi} \right]^2 + \frac{1}{2} C_2(4) \left[ \left( \frac{\alpha_s(M_b^2)}{\pi} \right)^2 - \left( \frac{\alpha_s(M_c^2)}{\pi} \right)^2 \right] \left. \right\} \\ &\times \left[ \frac{\alpha_s(s)}{\alpha_s(M_b^2)} \right]^{\gamma_0^{(5)}/\beta_0^{(5)}} \left\{ 1 + C_1(5) \left[ \frac{\alpha_s(s)}{\pi} - \frac{\alpha_s(M_b^2)}{\pi} \right] \right. \\ &+ \frac{1}{2} C_1^2(5) \left[ \frac{\alpha_s(s)}{\pi} - \frac{\alpha_s(M_b^2)}{\pi} \right]^2 + \frac{1}{2} C_2(5) \left[ \left( \frac{\alpha_s(s)}{\pi} \right)^2 - \left( \frac{\alpha_s(M_b^2)}{\pi} \right)^2 \right] \left. \right\}. \end{aligned} \quad (66)$$

For the running  $b$ -quark mass the same procedure is applied with a single evolution from  $M_b^2$  to  $s$ . The coefficients in Eq.66 are given by:

$$C_1(n_f) = \frac{\gamma_1^{(n_f)}}{\beta_0^{(n_f)}} - \frac{\beta_1^{(n_f)} \gamma_0^{(n_f)}}{\left( \beta_0^{(n_f)} \right)^2}, \quad (67)$$

$$C_2(n_f) = \frac{\gamma_2^{(n_f)}}{\beta_0^{(n_f)}} - \frac{\beta_1^{(n_f)} \gamma_1^{(n_f)}}{\left(\beta_0^{(n_f)}\right)^2} - \frac{\beta_2^{(n_f)} \gamma_0^{(n_f)}}{\left(\beta_0^{(n_f)}\right)^2} + \frac{\left(\beta_1^{(n_f)}\right)^2 \gamma_0^{(n_f)}}{\left(\beta_0^{(n_f)}\right)^3}. \quad (68)$$

The coefficients of the Beta and Gamma functions are:

$$\beta_0^{(n_f)} = \frac{1}{4} \left( 11 - \frac{2}{3} n_f \right), \quad (69)$$

$$\beta_1^{(n_f)} = \frac{1}{16} \left( 102 - \frac{38}{3} n_f \right), \quad (70)$$

$$\beta_2^{(n_f)} = \frac{1}{64} \left( \frac{2857}{2} - \frac{5033}{18} n_f + \frac{325}{54} n_f^2 \right), \quad (71)$$

$$\gamma_0^{(n_f)} = 1, \quad (72)$$

$$\gamma_1^{(n_f)} = \frac{1}{16} \left( \frac{202}{3} - \frac{20}{9} n_f \right), \quad (73)$$

$$\gamma_2^{(n_f)} = \frac{1}{64} \left\{ 1249 - \left[ \frac{2216}{27} + \frac{160}{3} \zeta(3) \right] n_f - \frac{140}{81} n_f^2 \right\}. \quad (74)$$

The renormalisation scale dependence of the coupling constant can be parameterised at 3-loop level as function of  $\Lambda_{\overline{\text{MS}}}^{(n_f)}$

$$\begin{aligned} \alpha_s(\mu) = & \frac{\pi}{\beta_0 \ln(\mu^2/\Lambda^2)} \left[ 1 - \frac{\beta_1}{\beta_0^2} \frac{\ln[\ln(\mu^2/\Lambda^2)]}{\ln(\mu^2/\Lambda^2)} + \frac{1}{\beta_0^2 \ln^2(\mu^2/\Lambda^2)} \times \right. \\ & \left. \times \left( \frac{\beta_1^2}{\beta_0^2} \left\{ \ln^2 \left( \frac{\mu^2}{\Lambda^2} \right) - \ln \left[ \ln \left( \frac{\mu^2}{\Lambda^2} \right) \right] - 1 \right\} + \frac{\beta_2}{\beta_0} \right) \right]. \end{aligned} \quad (75)$$

Technically, for a given input value of  $\alpha_s(M_Z)$ , Eq.75 is solved numerically for  $n_f = 5$  in order to obtain  $\Lambda_{\overline{\text{MS}}}^{(5)}$ . The scale parameters for  $n_f = 4$  and  $n_f = 3$ ,  $\Lambda_{\overline{\text{MS}}}^{(5)}$  and  $\Lambda_{\overline{\text{MS}}}^{(5)}$ , required for the evolution of  $\alpha_s$  to the scales of the quark pole masses  $M_b$  and  $M_c$ , are derived using the matching condition

$$\begin{aligned} \ln \left( \frac{\Lambda_{\overline{\text{MS}}}^{(n_f)}}{\Lambda_{\overline{\text{MS}}}^{(n_f-1)}} \right)^2 = & \beta_0^{(n_f-1)} \left\{ \left( \beta_0^{(n_f)} - \beta_0^{(n_f-1)} \right) L_M + \left( \frac{\beta_1^{(n_f)}}{\beta_0^{(n_f)}} - \frac{\beta_1^{(n_f-1)}}{\beta_0^{(n_f-1)}} \right) \ln L_M \right. \\ & - \frac{\beta_1^{(n_f-1)}}{\beta_0^{(n_f-1)}} \ln \frac{\beta_0^{(n_f)}}{\beta_0^{(n_f-1)}} + \frac{\beta_1^{(n_f)}}{\left( \beta_0^{(n_f)} \right)^2} \left( \frac{\beta_1^{(n_f)}}{\beta_0^{(n_f)}} - \frac{\beta_1^{(n_f-1)}}{\beta_0^{(n_f-1)}} \right) \frac{\ln L_M}{L_M} \\ & \left. + \frac{1}{\beta_0^{(n_f)}} \left[ \left( \frac{\beta_1^{(n_f)}}{\beta_0^{(n_f)}} \right)^2 - \left( \frac{\beta_1^{(n_f-1)}}{\beta_0^{(n_f-1)}} \right)^2 - \frac{\beta_2^{(n_f)}}{\beta_0^{(n_f)}} + \frac{\beta_2^{(n_f-1)}}{\beta_0^{(n_f-1)}} - \frac{7}{72} \right] \frac{1}{L_M} \right\}, \end{aligned} \quad (76)$$

with

$$L_M = \ln \frac{M_q^2}{\left(\Lambda_{\overline{\text{MS}}}^{(n_f)}\right)^2}. \quad (77)$$

## 4 Theoretical uncertainties for EW observables

The sensitivity of a given electroweak observable to  $\alpha_s$  originate on one side from the QCD corrections incorporated in the radiator functions and on the other side from the mixed EW $\otimes$ QCD corrections to the effective couplings. A measurement of  $\alpha_s$  using EW observables is hence subject to a systematic uncertainty stemming from missing higher orders in the perturbation series. The yet uncalculated higher orders are inherently difficult to access. A conventional method of estimating the perturbative uncertainty consists of a variation of the renormalisation scale  $\mu$ . The natural scale of the process is usually taken to be  $\sqrt(s)$ , and subsequently in the case of lineshape observables  $\mu$  is set to  $M_Z$ . This particular choice is not unambiguous [2], neither the range of variation which  $\mu$  should undergo. Following the procedure applied in analyses of  $e^+e^-$  event-shape variables, a range from  $M_Z/2 \leq \mu \leq 2M_Z$  is considered.

A variation of the renormalisation scale induces a change of the value of  $\alpha_s(\mu)$  as given in Eq.75. At NLO and beyond this change is compensated by a modification of the (N)NLO terms, resulting in a residual dependence at (N)NNLO. the details of the scale dependence of the radiator functions is discussed below.

The mixed  $\mathcal{O}(\alpha\alpha_s)$  corrections, being at leading order in QCD, are sensitive only to the change of  $\alpha_s(\mu)$ , without compensation at NLO. Therefore, the efective couplings are expected to have a strong scale dependence. In fact a few terms of the  $\mathcal{O}(\alpha\alpha_s^2)$  contribution, leading in  $m_t^2$ , are included in the expressions for  $\rho_Z^f$  and  $\kappa_Z^f$ , given in eqs. 21 and 26. It is debatable whether the explicit scale dependence of these terms should be taken into account, as they represent only part of the full NLO calculation. As a conservative estimate, the potential compensation of the scale dependence from these terms is neglected.

Given the overall small size of the EW  $\otimes$  QCD corrections, they do not contribute significantly to the scale dependence of the realistic observables.

In the present case of a complete NNLO calculation for the radiator functions, another estimate of missing higher orders can be deduced from the difference between the NNLO and the NLO result.

### 4.1 NNLO-NLO difference

The difference between the full NNLO result and the truncation at NLO can be used to assess the theoretical systematic uncertainty. Provided a fast convergence of the perturbation series, this difference can be regarded as a rough estimate of the 'true' error which would be the difference between the NNLO result and the complete theory. In fact this difference, containing the incomplete NLO result, should be seen as an uncertainty estimate of measurement based on the NLO theory, while an improved NNLO-based determination should have a smaller uncertainty. Technically, the reduction to NLO is straightforward, it is sufficient to drop the terms in Eqs.37-38 proportional to  $\alpha_s^3$ .

## 4.2 Renormalisation scale dependence

Dimensional regularisation introduces a renormalisation scale  $\mu$  at which the coupling constant is defined. Thereby, the coefficients in the expansion of  $R_{V,A}^q$  acquire an explicit dependence on this scale, which is only at all orders completely compensated by the scale dependence of  $\alpha_s(\mu)$ . For a NNLO calculation, the residual scale dependence is 3NLO. The nominal value of the  $\mu$  scale is usually set to the scale of the precess  $\mu^2 = s$ . A variation of  $\mu$  is conventionally taken as indicative of magnitude of missing higher orders [2]. The range of variation not unambiguously defined, though a customary convention is to estimate the perturbative uncertainty by changing  $x_\mu = \mu/\sqrt{s}$  in the range  $1/2 < x_\mu < 2$  [2].

The expression for  $R_{V,A}^q$  in Eqs.37 and 38 are valid only for  $\mu^2 = s$ , for different renormalisation scales terms proportional to powers of  $\ln \mu^2/s$  appear. For a generic power series of the type

$$R = \sum_{i=0}^n c_n \left( \frac{\alpha_s}{\pi} \right)^n, \quad (78)$$

the NLO coefficient  $c_2$  becomes a function of  $\mu$

$$c_2 \rightarrow c_2(\mu) = c_2 + \beta_0 c_1 \ln \frac{\mu^2}{s}. \quad (79)$$

It is important to note that two quantities depend on the renormalisation scale in Eqs.37 and 38: the coupling constant  $\alpha_s(\mu)$  (Eq.75) and the running masses  $m_q(\mu)$  (Eq.66).

In order to simplify the formulae for the scale dependence of the radiator functions, it is convenient to re-order Eqs.37 and 38 in terms of powers of the running masses:

$$R_{V,A}^q(\mu) = \sum_{f=q,\bar{q},c,b} \sum_{i=0}^3 \frac{m_f^{2i}(\mu)}{s^i} \sum_{j=0}^3 d_{ij,f}^{A,V} \bar{\alpha}_s^j, \quad (80)$$

where  $\bar{\alpha}_s = \frac{\alpha_s(\mu^2)}{\pi}$ . For each quark not only the mass of the actual quark, but also the mass the  $b$ - and  $c$ -quark masses intervene in the radiator functions, each with different coefficients. In the  $\overline{\text{MS}}$  scheme the expansion of the scale evolution of powers of the running masses reads as

$$\begin{aligned} m_q^2(s) &= m_q^2(\mu) \left( 1 + 2\gamma_0 L \bar{\alpha}_s + (\gamma_0 \beta_0 L^2 + 2\gamma_1 L + 2\gamma_0^2 L^2) \bar{\alpha}_s^2 \right. \\ &\quad \left. + \left[ \frac{2}{3} \gamma_0 \beta_0^2 L^3 + \gamma_0 \beta_0 L^2 + 2\gamma_2 L + 2\gamma_0^2 \beta_0 L^3 + 4\gamma_0 \gamma_1 L^2 + \frac{4}{3} \gamma_0^3 L^3 \right] \bar{\alpha}_s^3 \right), \end{aligned} \quad (81)$$

$$m_q^4(s) = m_q^4(\mu) \left( 1 + 4\gamma_0 L \bar{\alpha}_s + (2\gamma_0 \beta_0 L^2 + 4\gamma_1 L + 8\gamma_0^2 L^2) \bar{\alpha}_s^2 \right), \quad (82)$$

$$m_q^6(s) = m_q^4(\mu) (1 + 6\gamma_0 L \bar{\alpha}_s), \quad (83)$$

with  $L = \ln x_\mu^2$ . The new coefficients  $d_{i,j}^{A,V}$  are related to those of Eqs.37 and 38.

*Massless terms:*

$$d_{00,q}^V = 1 + \frac{3}{4} Q_q^2 \frac{\alpha(s)}{\pi}, \quad d_{00,q}^A = d_{00,q}^V, \quad (84)$$

$$d_{10,q}^V = 1 - \frac{1}{4} Q_q^2 \frac{\alpha(s)}{\pi} , \quad d_{10,q}^A = d_{10,q}^V, \quad (85)$$

$$d_{20,q}^V = C_{02} + C_2^t \left( \frac{s}{m_t^2} \right) , \quad d_{20,q}^A = C_{02} + (C_2^t - 2I_q^{(3)}\mathcal{I}^{(2)}) \left( \frac{s}{m_t^2} \right), \quad (86)$$

$$d_{30,q}^V = C_{03} , \quad d_{30,q}^A = C_{03} - 2I_q^{(3)}\mathcal{I}^{(2)}; \quad (87)$$

(88)

$m_q^2$  terms:

$$d_{02,q}^V = 0 , \quad d_{02,q}^A = C_{20}^A, \quad (89)$$

$$d_{12,q}^V = C_{21}^V , \quad d_{12,q}^A = C_{21}^A, \quad (90)$$

$$d_{22,q}^V = C_{22}^V , \quad d_{22,q}^A = C_{22}^A + 6 \left( 3 + \ln \frac{m_t^2}{s} \right) - 10 \frac{s}{m_t^2} \left( \frac{8}{81} + \frac{1}{54} \ln \frac{m_t^2}{s} \right), \quad (91)$$

$$d_{32,q}^V = C_{23}^V , \quad d_{32,q}^A = C_{23}^A, \quad (92)$$

$$d_{32,b}^V = d_{32,c}^V = C_{23} \quad , \quad d_{32,b}^A = d_{32,c}^A = C_{23}; \quad (93)$$

(94)

$m_q^4$  terms:

$$d_{04,q}^V = 0 , \quad d_{04,q}^A = C_{40}^A, \quad (95)$$

$$d_{14,q}^V = C_{41}^V , \quad d_{14,q}^A = C_{41}^A, \quad (96)$$

$$d_{24,q}^V = C_{42}^V + C_{42}^{V,L} \ln \frac{m_q^2(s)}{s} , \quad d_{24,q}^A = C_{42}^A + C_{42}^{A,L} \ln \frac{m_q^2(s)}{s}, \quad (97)$$

$$d_{24,b}^V = d_{24,b}^A = C_{42} - \ln \frac{m_b^2(s)}{s} , \quad d_{24,c}^V = d_{24,c}^A = C_{42} - \ln \frac{m_c^2(s)}{s} \quad (98)$$

$$d_{24,\hat{q}}^V = d_{24,\hat{q}}^A = 12; \quad (99)$$

(100)

$m_q^6$  terms:

$$d_{06,q}^V = 8 , \quad d_{06,q}^A = 0, \quad (101)$$

$$d_{16,q}^V = \frac{16}{27} \left( 155 + 6 \ln \ln \frac{m_q^2(s)}{s} \right) , \quad d_{16,q}^A = 0. \quad (102)$$

(103)

Finally, to get the renormalisation scale dependence of the radiator functions, the terms of the type  $m_q^j(s) \sum_i d_{ij} \alpha_s^i(s)/pi$  in Eq.80, dropping for clarity the axial-vector/vector and flavour indices, have to be replaced by the following expressions:

$$\begin{aligned} \sum_j d_{0j} \frac{\alpha_s^j(s)}{\pi} &\rightarrow d_{00} + d_{10} \bar{\alpha}_s + (d_{20} + d_{10} \beta_0 L) \bar{\alpha}_s^2 \\ &\quad + (d_{30} + (d_{10} \beta_1 + 2d_{20} \beta_0) + d_{10} \beta_0^2 L^2) \bar{\alpha}_s^3, \end{aligned} \quad (104)$$

$$m_q^2(s) \sum_j d_{j2} \frac{\alpha_s^j(s)}{\pi} \rightarrow m_q^2(\mu) \left[ d_{02} + (d_{12} + 2d_{02} \gamma_0 L) \bar{\alpha}_s \right. \quad (105)$$

$$\begin{aligned}
& + (d_{12}\beta_0 L + d_{22} + 2d_{12}\gamma_0 L + d_{02}\gamma_0\beta_0 L^2 + 2d_{02}\gamma_1 L + 2d_{02}\gamma_0^2 L^2) \bar{\alpha}_s^2 \\
& + \left( d_{12}\beta_0^2 L^2 + d_{12}\beta_1 L + d_{32} + 2d_{22}\beta_0 L + \frac{2}{3}d_{02}\gamma_0\beta_0^2 L^3 + d_{02}\gamma_0\beta_1 L^2 \right. \\
& \left. + 2d_{02}\gamma_1\beta_0 L^2 + 2d_{02}\gamma_2 L + 2d_{02}\gamma_0^2\beta_0 L^3 + 4d_{02}\gamma_0\gamma_1 L^2 + \frac{4}{3}d_{02}\gamma_0^3 L^3 \right. \\
& \left. + 3d_{12}\gamma_0\beta_0 L^2 + 2d_{22}\gamma_0 L + 2d_{12}\gamma_1 L + 2d_{12}\gamma_0^2 L^2 \right) \bar{\alpha}_s^3,
\end{aligned}$$

$$m_q^4(s) \sum_j d_{j4} \frac{\alpha_s^j(s)}{\pi} \rightarrow m_q^4(\mu) \left[ d_{04} + (d_{14} + 4d_{04}\gamma_0 L) \bar{\alpha}_s \right. \\
\left. (d_{14}\beta_0 L + d_{24} + 2d_{04}\gamma_0\beta_0 L^2 + 4d_{04}\gamma_1 L + 8d_{04}\gamma_0^2 L^2 + 4d_{14}\gamma_0 L) \bar{\alpha}_s^2 \right] \quad (106)$$

$$m_q^6(s) \sum_j d_{j6} \frac{\alpha_s^j(s)}{\pi} \rightarrow m_q^6(\mu) \left[ d_{06} + (d_{16} + 6d_{06}\gamma_0 L) \bar{\alpha}_s \right] \quad (107)$$

The dependence of the radiator functions on the renormalisation scale  $\ln x_\mu$  for a fixed input value of  $\alpha_s(M_Z)$  is shown for each quark flavour in fig. 4. The shape of the scale dependence of  $R_V^q$  is almost identical for all flavours, except a small quark mass modification for the b-quark. The overall scale dependence of the axial-vector component  $R_A^q$  is twice as large as the one of  $R_V^q$ . As already observed for the dependence on  $\alpha_s$  in fig.3, the shape of  $R_A^q$  is clearly different for up- and down-type quarks. Considering the range of variation in  $x_\mu$  from  $1/2$  to  $2$ , corresponding to a range in  $\ln x_\mu$  from  $-0.7$  to  $0.7$ , it appears that largest deviation from the nominal point at  $\ln x_\mu = 0$  is not always obtained at the endpoints, but sometimes at before. Therefore, when assessing the uncertainty for the observables studied in the following, the endpoints of  $\ln x_\mu$  ( $\ln x_\mu^-$  and  $\ln x_\mu^+$ ) have been chosen to correspond to the largest change in the observables, within the pre-defined range  $|\ln x_\mu| < 0.7$ .

The dependence of the effective couplings on  $\ln x_\mu$  is shown in fig.5. Shown are the absolute value of  $\rho_Z^f$  and its square for  $\kappa_Z^f$  as they appear in the expressions for the widths. The structure of the couplings dependence is rather different from the radiator functions, driven uniquely by the scale dependence of  $\alpha_s(\mu)$ . In the absence of the cancellation by higher order terms, the effective couplings don't exhibit any maxima or minima. The dependence of  $\rho_Z^f$  is the same for all quarks and leptons, except the b-quark. For  $|\kappa_Z^f|^2$  a much stronger dependence is observed, scaling with the electric charge squared.

Turning to the widths, for hadronic final states both the effective couplings and the radiator functions discussed above contribute to scale dependence. For the leptonic widths only the effective couplings depend on the renormalisation scale through the  $\mathcal{O}(\alpha\alpha_s)$  corrections. The relative magnitude of contributions is given by the formulae for the widths, eq.5 for the leptons and eq.6 for the quarks. The scale dependence of the widths and of the realistic observables are shown in fig. 6.

The shape of the scale dependence for the widths depends on the fermion type. For the u- and c-quark a maximum is found close to  $\ln x_\mu = 1$ , and variations of  $\ln x_\mu$  in any direction entail a decrease of the width. The partial widths into d- and s-quarks increase monotonically from  $\ln x_\mu = -0.7$  to  $\ln x_\mu = 0.7$ , similarly for the width of the b-quark, albeit with a flatter shape. The total hadronic widths of the  $Z$  boson emerges as

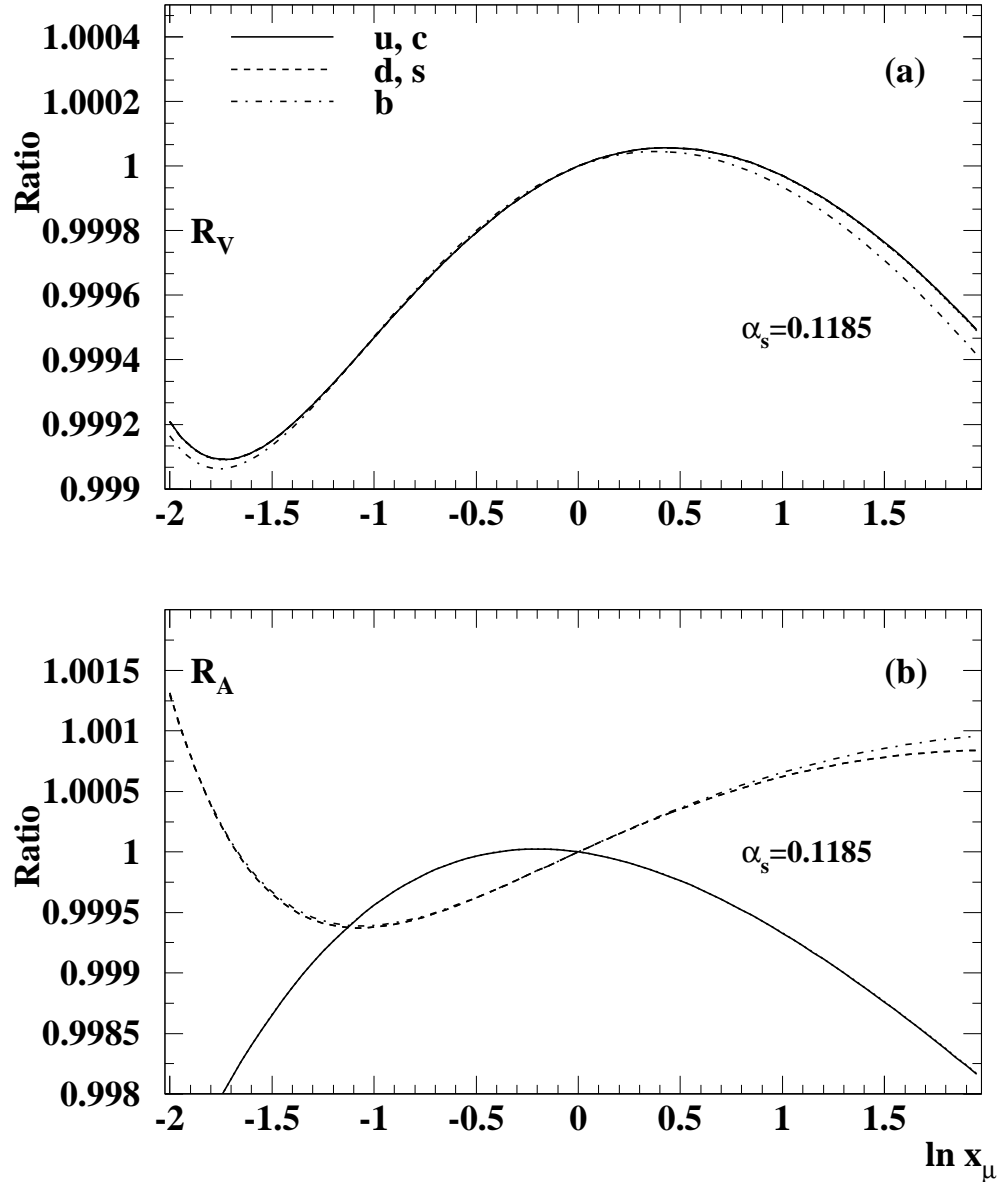


Figure 4: Dependence of the radiator functions on the renormalisation scale. The vector correction  $R_V^q$  (a) and the axial vector correction  $R_A^q$  (b) are shown for the quarks  $q = u, d, s, c, b$  as function of  $\log x_\mu$ , normalised to their value at  $x_\mu = 1$ .

sum of the quarkonic contributions, leading to an average shape of its scale dependence. The scale dependence of the leptonic widths is clearly weaker than that of the quarkonic counterparts, but not negligible. In the central range of  $\ln x_\mu$  the leptonic width changes by about half the hadronic width's change. The sensitivity of  $\Gamma_l$  to the renormalisation scale arise through the  $\text{EW} \times \text{QCD}$  corrections, essentially those incorporated in  $\rho_Z^l$ .

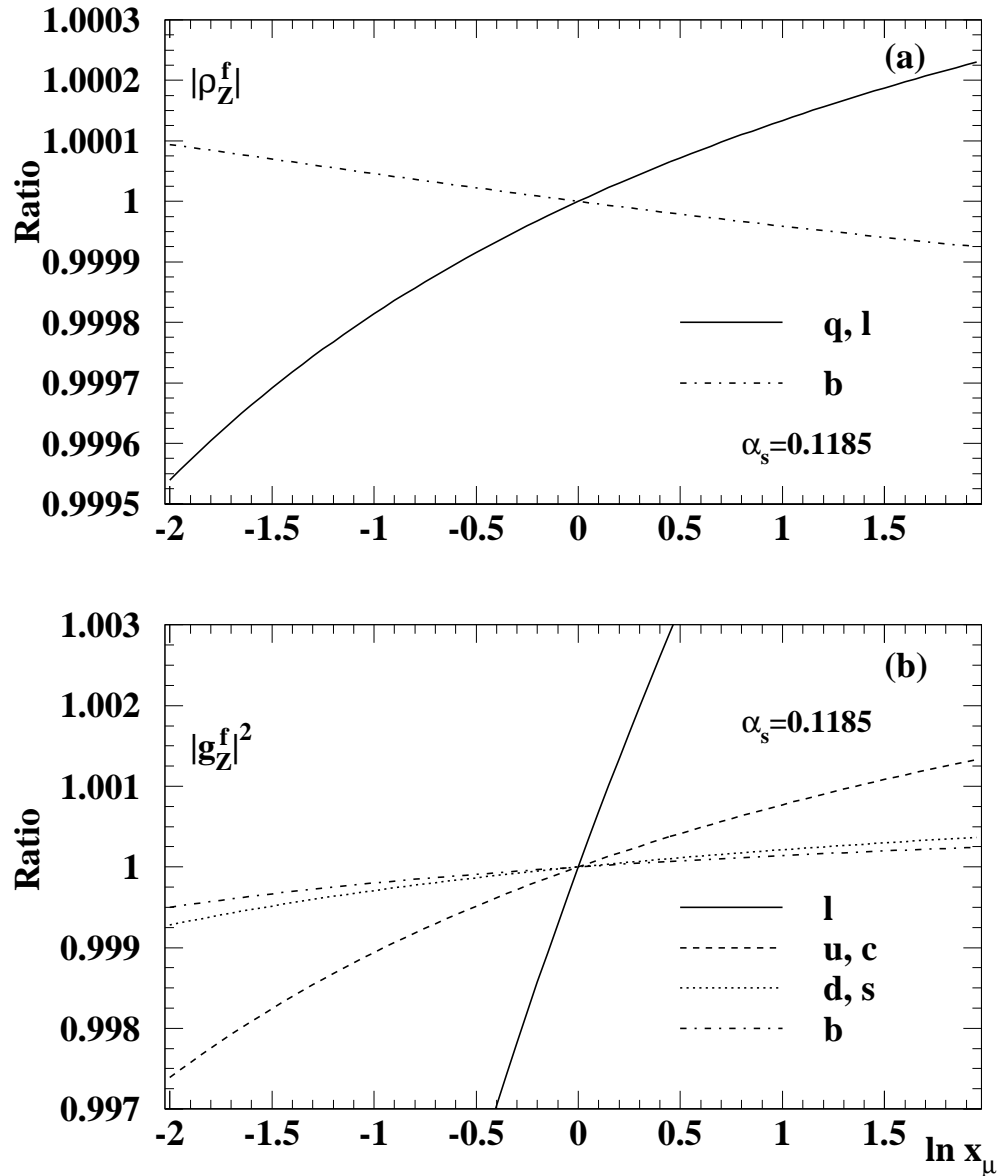


Figure 5: Dependence of the effective couplings  $|\rho_Z^f|$  (a) and  $|g_Z^f|^2$  (b) on the renormalisation scale.

## 5 Perturbative uncertainties for $\alpha_s$

In the context of global analyses of world electroweak data [1]  $\alpha_s(M_Z)$  is fit together with four other free parameters of the standard model:  $M_h^2/s$ ,  $M_Z$ ,  $m_t^2$  and  $\Delta\alpha_{had}^{(5)}$ . The correlation between  $\alpha_s$  and the other parameters is small. The observables included in the fit with a sizeable sensitivity to  $\alpha_s$  are  $R_Z$ ,  $\Gamma_Z$  and  $\sigma_h^0$ . The leptonic pole cross section  $\sigma_l^0$  is usually not included in the global fits although it has actually the best sensitivity through the inverse squared radiator functions. Alternatively, a single observable like  $\sigma_l^0$  may be selected and  $\alpha_s$  determined in a single parameter fit with the other parameters

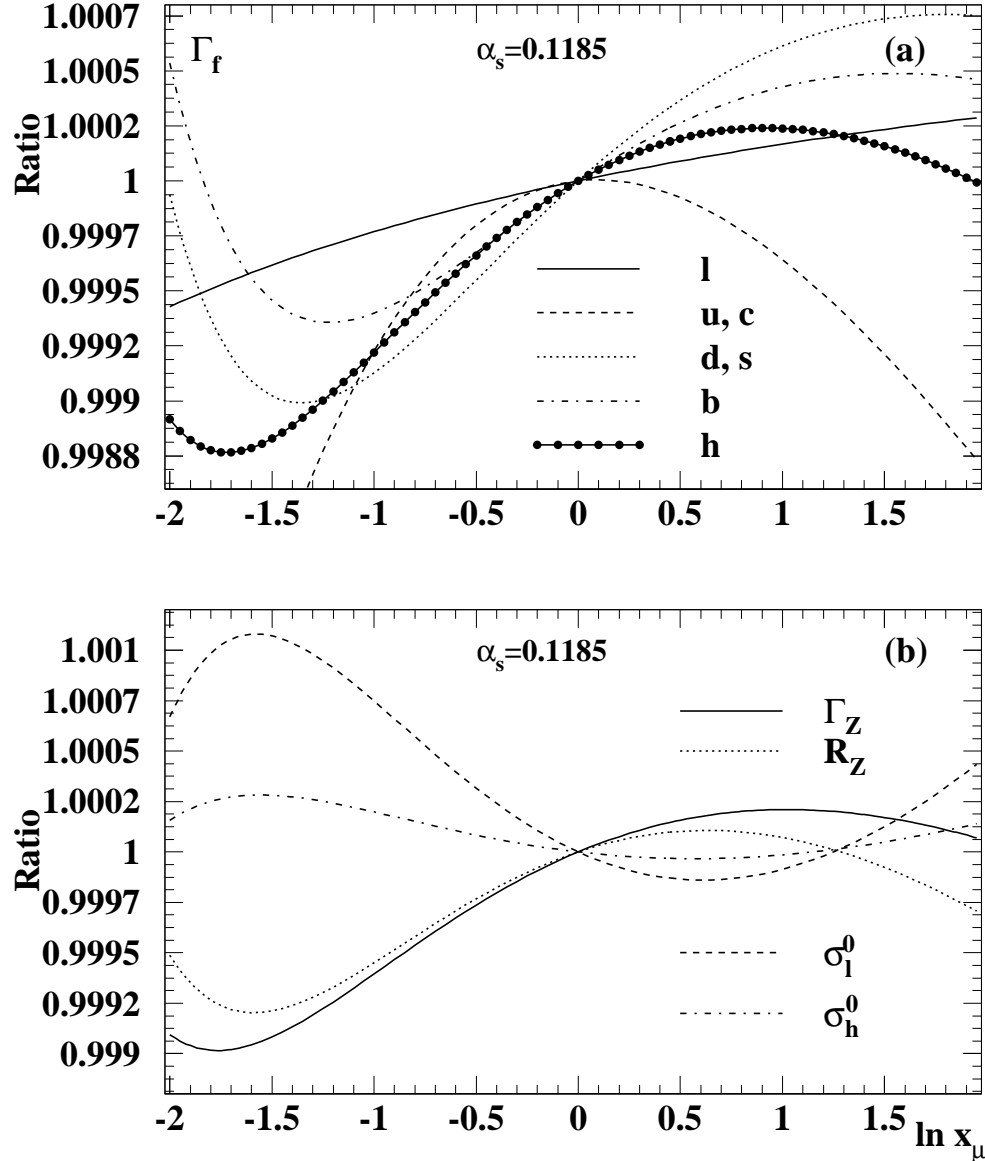


Figure 6: Dependence of the widths (a) and selected realistic observables (b) on the renormalisation scale for  $\alpha_s(M_Z) = 0.1185$ .

being set to their measurement, in order to investigate the dependence of  $\alpha_s$  on the Higgs mass.

Having in mind this scenario, the procedure is to determine in a first step the perturbative uncertainty for measurements of  $\alpha_s$  using single selected observables and to estimate in a second step the uncertainty for a global fit including several variables.

The basic principle for the uncertainty estimation was developed in [2]: the systematic uncertainty for a given observable and fixed value of  $\alpha_s(M_Z)$  (i.e. as obtained from a fit to this observable) is evaluated in the theory by variation of the renormalisation scale  $x_\mu^- < x_\mu < x_\mu^+$ . The change of the observables under the scale variation can also be

generated by a variation of the input value of  $\alpha_s$  at fixed  $x_\mu = 1$ . This procedure leads in general to two alternative values of  $\alpha_s$  corresponding to the changes of the observable for  $x_\mu^-$  and  $x_\mu^+$ . The difference between the nominal value of  $\alpha_s$  and these two alternatives set finally the perturbative uncertainty of  $\alpha_s$ .

The uncertainty itself depends on the type of observable and on the input value of  $\alpha_s$ . At NNLO the size of the perturbative uncertainty is scaling with  $\alpha_s^4$ . It is instructive to consider the uncertainty for  $\alpha_s$  for the pseudo-observable widths in a first step, in order to understand their contribution to realistic observables. The systematic uncertainties are shown in fig. 7 as function of the input value of  $\alpha_s$  in a relevant range from 0.11 to 0.13. As expected from the scale uncertainty of the width itself, there are large differences between the uncertainties of  $\alpha_s$  determined using the widths of up- and down-type quarks. Given the shape of the scale uncertainty for the width of the u- and c-quark, the resulting uncertainty of  $\alpha_s$  is essentially one-sided only. Also for the other widths a certain asymmetry in the uncertainty is observed, the positive (upward) uncertainty is generally larger than the negative (downward). This asymmetry may well be a technical artefact of the scale variation prescription, and conservatively the maximum of the positive and negative uncertainty is assigned as symmetric uncertainty. For selected input values of  $\alpha_s(M_Z)$  the symmetrised uncertainties are given in Table 1.

Table 1: Systematic perturbative uncertainties for measurements of  $\alpha_s$  from EW observables. The symmetric uncertainty is given by the maximum of upward and downward uncertainties obtained by a renormalisation scale variation.

$\alpha_s(M_Z)$	0.110	0.115	0.120	0.125	0.130
$\Gamma_u$	0.00074	0.00084	0.00095	0.00107	0.00121
$\Gamma_{d,s}$	0.00204	0.00244	0.00291	0.00345	0.00408
$\Gamma_c$	0.00072	0.00081	0.00092	0.00104	0.00118
$\Gamma_b$	0.00103	0.00127	0.00154	0.00187	0.00225
$\Gamma_h$	0.00123	0.00143	0.00168	0.00199	0.00232

The uncertainty of  $\alpha_s$  determined from realistic electroweak observables is shown in fig.8. The largest uncertainty is observed in the case of  $\Gamma_Z$ , which is directly proportional to the product of effective couplings and radiator functions. The other observables yield uncertainties reduced by a factor of two, with little differences between the observables. In  $R_Z$  the widths appear linearly in nominator and denominator, in  $\sigma_l^0$  and  $\sigma_h^0$  quadratic combinations of leptonic, hadronic and total widths of the Z boson interplay. As a consequence the scale dependence of the effective couplings and/or the radiator functions cancel to some extend in the ratio.

In the context of global analyses of electroweak data [1] several observables are included, but only  $R_Z$ ,  $\Gamma_Z$  and  $\sigma_h^0$  have a sizeable sensitivity to  $\alpha_s$ . Effectively, these three observables determine  $\alpha_s$  and the perturbative uncertainty of  $\alpha_s$  is bound to be an average of their individual contribution. The exact weights of each variable to the determination of  $\alpha_s$  and subsequently to its perturbative uncertainties can not be determined in the framework of the present work. In order to derive nonetheless an estimate of the perturbative uncertainty from a global fit, an unweighted average  $\Delta$  of

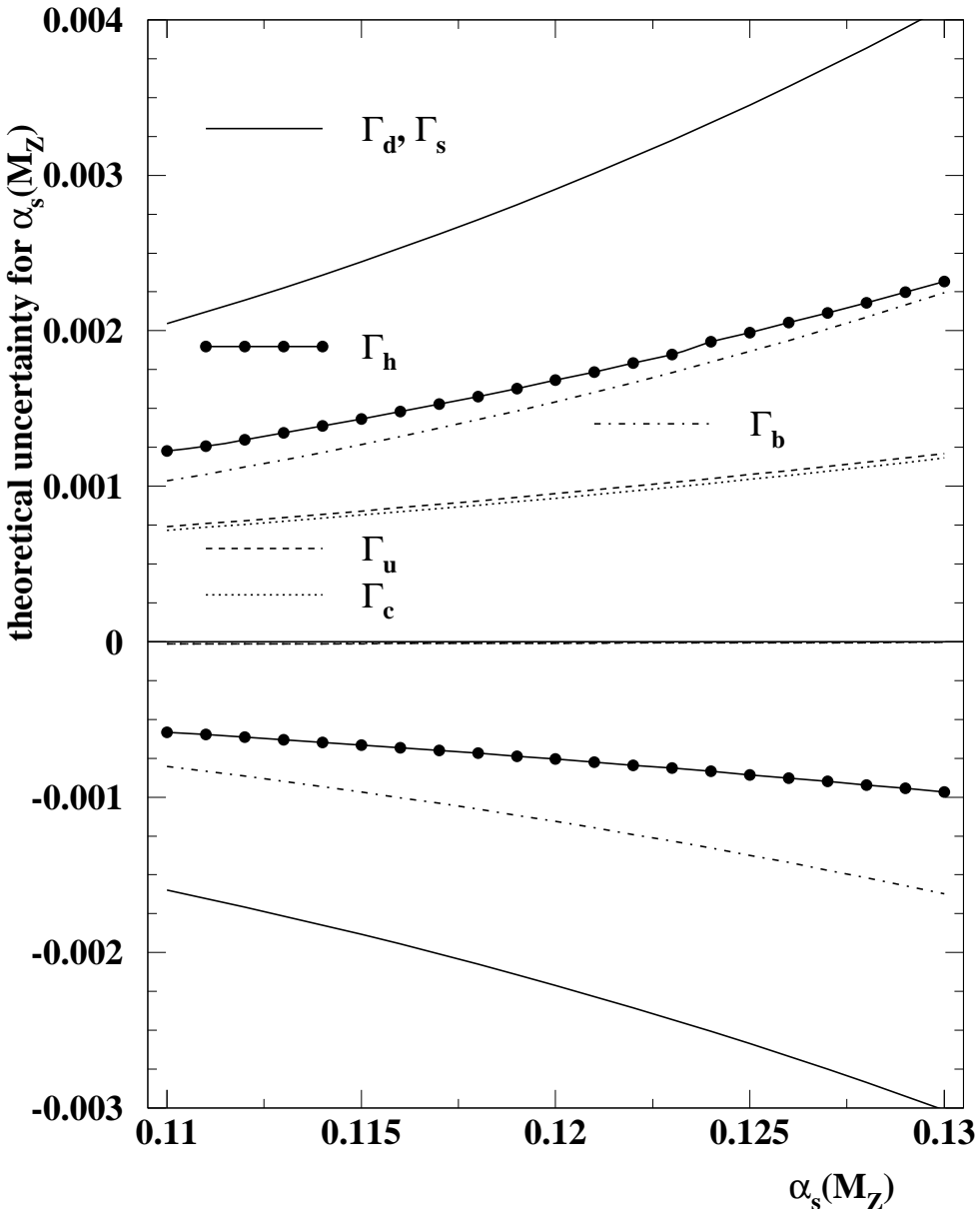


Figure 7: Positive and negative contributions to the perturbative systematic uncertainty of  $\alpha_s(M_Z)$  determined from various partial widths of the Z boson.

the contributions from  $R_Z$ ,  $\Gamma_Z$  and  $\sigma_h^0$  is taken. The uncertainty of this procedure is given by the largest difference with respect to the individual contributions, in practice the uncertainty from  $\Gamma_Z$  sets the upper and  $\sigma_h^0$  the lower limit. In Table 2 the symmetric perturbative are summarised for the realistic observables and the unweighted average in a narrow range around 0.119. The possible variations for the combined uncertainty are also given as  $\Delta^+$  for the upper and  $\Delta^-$  for the lower bound.

For a value of  $\alpha_s(M_Z)$  the perturbative uncertainty ranges from  $\pm 0.00104$  for  $\sigma_h^0$  to  $\pm 0.00189$  for  $\Gamma_Z$ , with an unweighted average of  $\pm 0.00136$ .

The dependence of the symmetric uncertainty on the input value of  $\alpha_s(M_Z)$  as

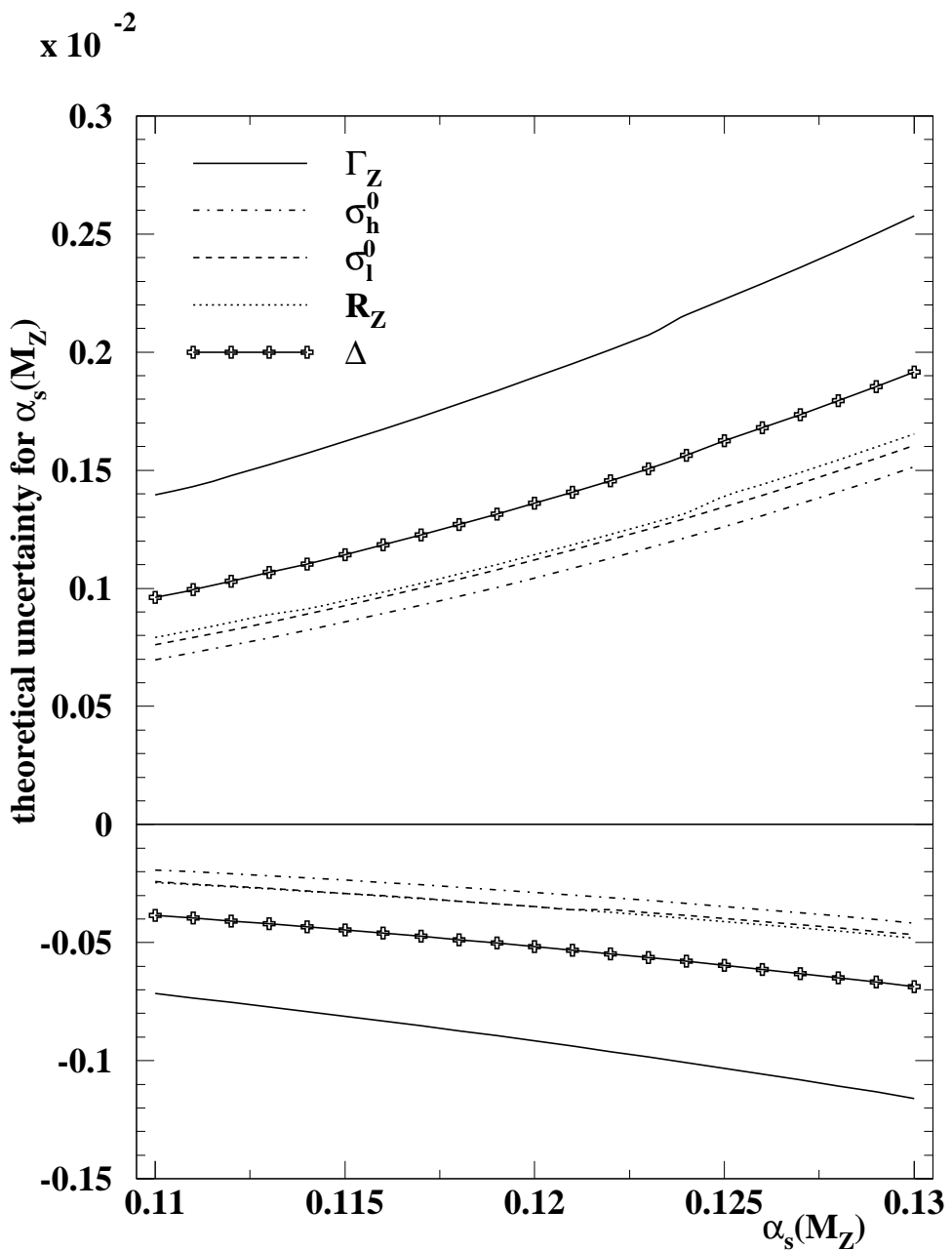


Figure 8: Systematic perturbative uncertainties for measurements of  $\alpha_s$  using the EW observables  $\Gamma_Z$ ,  $R_Z$ ,  $\sigma_l^0$  and  $\sigma_h^0$  as function of the input value of  $\alpha_s(M_Z)$ . The quantity  $\Delta$  denotes an unweighted average of the uncertainty for  $\Gamma_Z$ ,  $R_Z$  and  $\sigma_h^0$ , relevant for global analyses of electroweak data.

obtained from a global fit can smoothly be parameterised to form  $a + b \cdot \alpha_s(M_Z)^4$ . The parameterisation, valid between  $0.11 \leq \alpha_s(M_Z) \leq 0.13$ , allows for an interpolation of the uncertainty between calculated points. The parameters  $a$  and  $b$  are given for each observable in Table 2. The result of the parameterisation is compared in fig.9 to the exact calculation, which is reproduced to good accuracy.

Table 2: Systematic perturbative uncertainties for measurements of  $\alpha_s$  from EW observables. The symmetric uncertainty is given by the maximum of upward and downward uncertainties obtained by a renormalisation scale variation.

$\alpha_s(M_Z)$	0.118	0.119	0.120	0.121	0.122	$a$	$b$
$\Gamma_Z$	0.00178	0.00184	0.00189	0.00195	0.00201	$1.29 \cdot 10^{-4}$	8.55
$\sigma_h^0$	0.00097	0.00100	0.00104	0.00108	0.00113	$-1.62 \cdot 10^{-4}$	5.83
$\sigma_l^0$	0.00104	0.00108	0.00112	0.00116	0.00121	$-1.31 \cdot 10^{-4}$	6.05
$R_Z$	0.00106	0.00110	0.00114	0.00118	0.00123	$-1.23 \cdot 10^{-4}$	6.18
$\Delta$	0.00127	0.00131	0.00136	0.00141	0.00146	$-5.35 \cdot 10^{-5}$	6.85
$\Delta^+$	+0.00051	+0.00053	+0.00053	+0.00054	+0.00055		
$\Delta^-$	-0.00030	-0.00031	-0.00032	-0.00033	-0.00033		

## 6 Conclusions

A new method has been presented for the perturbative uncertainties at NNLO of measurements of  $\alpha_s$  obtained from global analyses of precision electroweak data. The systematic uncertainties are obtained by a variation of the renormalisation in the calculations of final state QCD and mixed QCD $\otimes$ EW corrections for the electroweak observables included in the global analyses used to determine  $\alpha_s$  and other Standard Model parameters. Individual contributions to the renormalisation scale dependence have been studied in detail and the resulting uncertainty has been calculated for the widths of the Z boson into different quark flavours and leptons. For electroweak observables used to constrain the Standard Model and determine  $\alpha_s(M_Z)$  a the corresponding perturbative uncertainty of  $\alpha_s(M_Z) = 0.12$  is estimated to be between  $\pm 0.0011$  and  $\pm 0.0019$ , in average  $\pm 0.0014$ . The determination of  $\alpha_s$  at NNLO from electroweak data is one of most precise measurements of  $\alpha_s(M_Z)$ . Its precision is dominated by experimental effects yielding a relative uncertainty of about 3%, while perturbative uncertainties contribute only 1.4%.

## Acknowledgements

The author would like to S. Bethke who has initially raised the issue of the perturbative uncertainties in this context. The author is indebted to G.P. Salam and R. Harlander for providing the essential ingredient on the renormalisation scale variation in presence of running quark masses. This article would not have been completed without the expertise provided by M. Grünwald on the topic of precision electroweak measurements and constraints on the Standard Model.

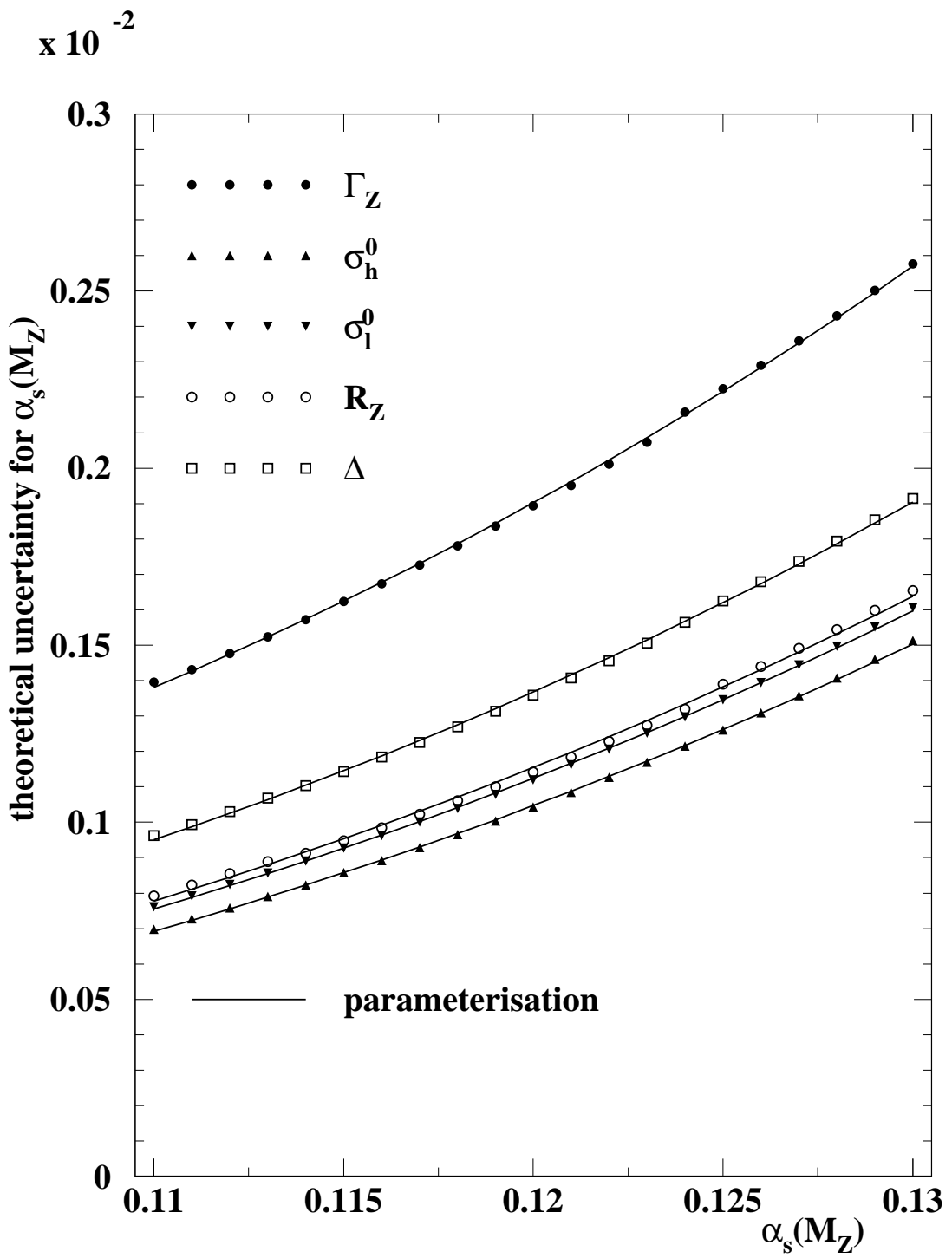


Figure 9: Symmetrised systematic perturbative uncertainties for measurements of  $\alpha_s$  using the EW observables. The quantity  $\Delta$  denotes an unweighted average of the uncertainty for  $\Gamma_Z$ ,  $R_Z$  and  $\sigma_h^0$ , relevant for global analyses of electroweak data. The symbols show the exact calculation and the lines represent the result of the parameterisation.

## References

- [1] The LEP Collaborations ALEPH, DELPHI, L3, OPAL, the LEP Electroweak working group, the SLD Electroweak and Heavy Flavour Working group, “*A Combination of preliminary Electroweak Measurements and constraints on the Standard Model*”, hep-ex/0412015
- [2] R. Jones, M. Ford, G.P. Salam, H. Stenzel and D. Wicke “*Theoretical uncertainties on  $\alpha_s$  from event-shape variables in  $e^+e^-$  annihilations*”, JHEP **12** (2003) 007.
- [3] D. Bardin et al., “*ZFITTER v.6.21 - A Semi-Analytical Program for Fermion Pair Production in  $e^+e^-$  Annihilation*”, Comput. Phys. Commun. **133** (2001) 229.
- [4] A. Czarnecki and J. H. Kühn, Phys. Rev. Lett. **77** (1996) 3955–3958.
- [5] R. Harlander, T. Seidensticker, and M. Steinhauser, Phys. Lett. **B426** (1998) 125–132.
- [6] M. Steinhauser, Phys. Lett. **B429** (1998) 158.
- [7] H. Burkhardt and B. Pietrzyk, Phys. Lett. **B513** (2001) 46.
- [8] L. Avdeev, J. Fleischer, S. Mikhailov, and O. Tarasov, Phys. Lett. **B336** (1994) 560–566, E: *ibid.*, **B 349** (1995) 597;  
K. G. Chetyrkin, J. H. Kühn, and M. Steinhauser, Phys. Lett. **B351** (1995) 331–338.
- [9] A. Akhundov, D. Bardin, and T. Riemann, “Electroweak one loop corrections to the decay of the neutral vector boson”, Nucl. Phys. **B276** (1986) 1.
- [10] J. Fleischer, O. V. Tarasov, F. Jegerlehner, and P. Raczka, Phys. Lett. **B293** (1992) 437–444.
- [11] J. Fleischer, O. V. Tarasov, and F. Jegerlehner, Phys. Lett. **B319** (1993) 249–256.
- [12] B. A. Kniehl, Nucl. Phys. **B347** (1990) 86.
- [13] K. G. Chetyrkin, A. L. Kataev, and F. V. Tkachev, Phys. Lett. **B85** (1979) 277.
- [14] M. Dine and J. Sapirstein, Phys. Rev. Lett. **43** (1979) 668.
- [15] W. Celmaster and R. J. Gonsalves, Phys. Rev. Lett. **44** (1980) 560.
- [16] S. G. Gorishny, A. L. Kataev, and S. A. Larin, Phys. Lett. **B273** (1991) 141–144.
- [17] K. Chetyrkin, J. Kühn, and A. Kwiatkowski, “QCD corrections to the  $e^+e^-$  cross-section and the Z boson decay rate”, in *Reports of the Working Group on Precision Calculations for the Z Resonance*, report CERN 95–03 (1995) (D. Bardin, W. Hollik, and G. Passarino, eds.), pp. 175–263.
- [18] M. Consoli, W. Hollik, and F. Jegerlehner, “Electroweak radiative corrections for Z physics”, in *Proc. of Workshop on Z Physics at LEP, Geneva, Switzerland, Feb 20-21 and May 8-9, 1989*, report CERN 89–08 (1989)